

Mechanical Unfolding Pathways of the Enhanced Yellow Fluorescent Protein Revealed by Single Molecule Force Spectroscopy*

Received for publication, October 20, 2006 Published, JBC Papers in Press, November 2, 2006, DOI 10.1074/jbc.M609890200

Raul Perez-Jimenez¹, Sergi Garcia-Manyes², Sri Rama Koti Ainavaru, and Julio M. Fernandez³

From the Department of Biological Sciences, Columbia University, New York, New York 10027

We used single molecule force spectroscopy to characterize the mechanical stability of the enhanced yellow fluorescent protein (EYFP) (a mutant form of the green fluorescent protein (GFP)) and two of its circularly permuted variants. In all three constructs, we found two main unfolding peaks; the first corresponds to a transition state placed close to the termini and the second to a transition state placed halfway through the molecule. We attribute the second transition state to the shear rupture of the β 1- and β 6-strands, which we verified by introducing a point mutation in this region. Although both unfolding peaks were observed in all three EYFP variants, their relative frequency of occurrence varied. Our results demonstrated that the mechanical unfolding pathways in EYFP could be deciphered through the use of circular permutation.

Green fluorescent protein (GFP)⁴ from the jellyfish *Aequorea victoria* has been used extensively in biology as a marker for gene expression (1) and reporters of the local cellular environment (2). We determined that it would be useful to extend the capabilities of GFP proteins to allow them to sense and report mechanical force through their fluorescence. An in-depth knowledge of the mechanical properties of GFP proteins was therefore required as a first step in the development of GFP-based mechanical sensors.

The GFP family of proteins contain 238 residues, forming an 11-stranded β -barrel structure (2–4) (Fig. 1) with the chromophore formed by autocatalytic cyclization of the residues in positions 65–67 located in the central helix (5). Several circular permutations of GFP have been reported in the literature (6, 7) and have also been shown to be fluorescent. Circular permutants of GFP are convenient, because they allow us to selectively apply force from different positions of the molecule, such that force dis-

tributes differently within the β -barrel structure. This may prove useful in future GFP designs, where it may be desirable to control the sensitivity of the chromophore to an applied force.

In previous work using single molecule force spectroscopy, Dietz and Rief (8) demonstrate that the wild type form of GFP (wt-GFP) mechanically unfolds through two short-lived intermediate states, the first one being related to the unfolding of the small α -helix close to the N terminus, giving rise to an increment in contour length of 3.2 nm, and the second one being related to the detachment of a β -strand from the barrel associated with an additional contour length increase of 6.8 nm. In addition, they show that the wt-GFP unfolds at \sim 100 pN. In similar atomic force microscopy studies, Hara and co-workers (9–11), using a circular permutant of GFP (9–11), detected one additional mechanically stable intermediate at an extension of \sim 50 nm (counting from the resting length of the molecule). Surprisingly, these studies show that the circular permutants of GFP are far more mechanically stable than the wild type form, requiring over 200 pN to unfold (9, 10). However, these studies were done without the benefit of a mechanical fingerprint, making it more difficult to unambiguously detect the unfolding of single GFP proteins.

The enhanced yellow fluorescent protein (EYFP) is a particularly useful variant of GFP. EYFP is structurally equivalent to GFP with five additional mutations (S65G, V68L, Q69K, S72A, and T203Y) that increase the emission wavelength and the brightness (2, 12). To critically examine the mechanical unfolding pathway of EYFP and correlate our results with the structural features of the molecule, we have studied the mechanical stability of wild type EYFP and two of its circular permutants (cp145-EYFP and cp174-EYFP). In all of our protein constructs, we have engineered mechanical fingerprints by bracketing EYFP with tetrameric or pentameric handles made of the I27 module of human cardiac titin (Fig. 2A) (8). This approach permits a direct determination of the unfolding distances that can then be related to the position of the mechanical transition states in the tertiary structure of the EYFP molecule.

EXPERIMENTAL PROCEDURES

Construction of the (I27)_{4,5}-EYFP(I27)₄ Polyproteins—In the case of the wild type form, the polyprotein was constructed with handles composed of four repeats of the I27 modules of human cardiac titin (Fig. 2A). For the circularly permuted forms, a tetramer and a pentamer of I27 were used as handles. As previously, we followed a multistep cloning procedure to construct the I27 handle polyproteins and the subsequent insertion of a

* This work was supported by National Institutes of Health Grants HL66030 and HL61228 (to J. M. F.). The costs of publication of this article were defrayed in part by the payment of page charges. This article must therefore be hereby marked "advertisement" in accordance with 18 U.S.C. Section 1734 solely to indicate this fact.

¹ Postdoctoral fellow of the Spanish Ministry of Education and Science.

² Recipient of a postdoctoral fellowship from the Generalitat de Catalunya (NANO program).

³ To whom correspondence should be addressed: Dept. of Biological Sciences, Columbia University, 1011A Fairchild Ctr., 1212 Amsterdam Ave., MC 2449, New York, NY 10027. Tel.: 212-854-9474; Fax: 212-854-4619; E-mail: jfernandez@columbia.edu.

⁴ The abbreviations used are: GFP, green fluorescent protein; EYFP, enhanced yellow fluorescent protein; I27, 27th immunoglobulin domain of human cardiac titin; wt, wild type; pN, piconewton(s); cp, circular permutant.

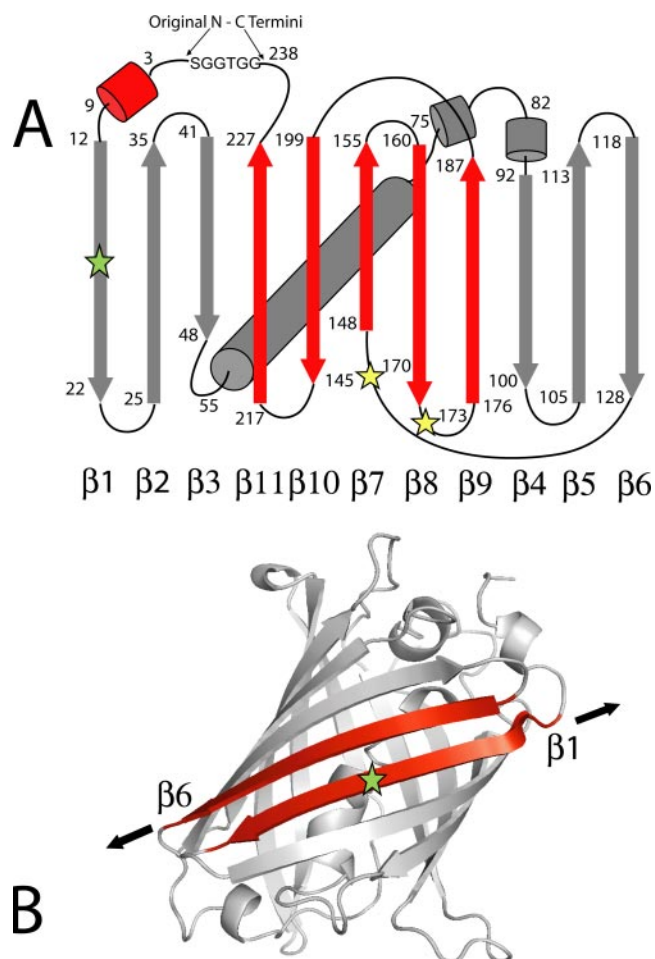


FIGURE 1. *A*, schematic representation of the β -structure of EYFP. The *yellow stars* show the position of the new N and C termini for the two circularly permuted forms obtained in positions 144/145 and 173/174. The *numbering* corresponds to the wt-EYFP sequence. *B*, representation of the β -barrel of YFP (Protein Data Bank code 1yfp) generated using Pymol. β 1- and β 6-strands are shown in *red*. The *black arrows* show the direction along which the force is applied, thus giving rise to the rupture of the two β -strands in a shear mechanism. The *green star* indicates the position 89 in cp174-EYFP where a glutamate to proline mutation (E89P) was engineered.

single EYFP monomer in between the handles (13). Circular permutations in the EYFP monomer were made according to a procedure described elsewhere (6). In the circular permuteds, the position of the termini is changed with respect to the wild type form. The original termini are closed by adding a linker composed of six residues (SGGTGG). The EYFP DNA was purchased from Clontech. In PCR amplifications, the QuikChange site-directed mutagenesis kit from Stratagene was used. The same kit was used to introduce a point mutation in the circularly permuted form cp174-EYFP. The proteins were expressed in recombination-defective strain BLR (DE3) from Novagene. The His₆-tagged proteins were purified first by Co²⁺ affinity chromatography using Talon resin from BD Biosciences and then by size exclusion chromatography using a prepacked Superdex 200 HR 10/30 column from GE Healthcare. The proteins were stored in 10 mM HEPES, 150 mM NaCl, and 1 mM EDTA, pH 7.2, and allowed to adsorb onto a freshly evaporated gold coverslip before the pulling experiments.

Single Molecule Force Microscopy—The details of our custom-made atomic force microscopy apparatus have been

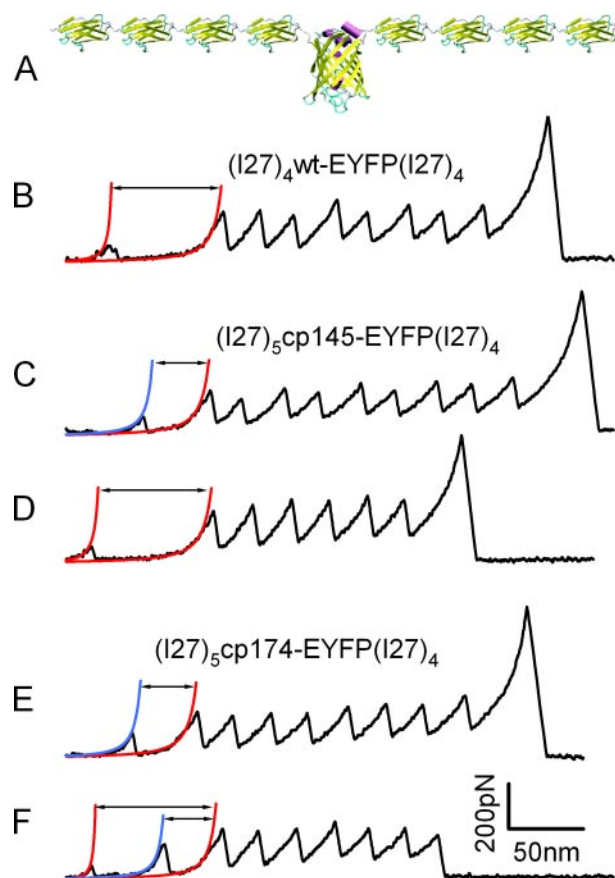


FIGURE 2. *A*, diagram of the polyprotein construct used with all three variants of EYFP. The EYFP protein is bracketed by two I27 handles that serve as single molecule fingerprints. *B*, force extension trace for $(I27)_4$ wt-EYFP $(I27)_4$ showing an wt-EYFP unfolding peak 79 ± 4 nm before the sequential unfolding of the I27 handles (equally spaced sawtooth pattern with eight unfolding peaks). *A* sawtooth pattern of five or more I27 unfolding peaks ensures that the EYFP molecule was unfolded. Shown are traces obtained from $(I27)_5$ cp145-EYFP $(I27)_4$ showing unfolding peaks at 40 ± 3 nm (*C*) and 84 ± 4 nm (*D*) prior to the I27 unfolding peaks. Shown are traces obtained from $(I27)_5$ cp174-EYFP $(I27)_4$ showing an unfolding peak at 41 ± 2 nm (*E*) and two unfolding peaks at 41 ± 2 nm and 90 ± 4 nm (*F*). The contour lengths were measured by fitting the data with the worm-like chain model of polymer elasticity (*red and blue lines*).

described elsewhere (14). The control of the atomic force microscopy head is carried out by data acquisition cards (6052E and 6703) from National Instrument (Austin, TX). The cantilevers (Si₃N₄) from Veeco were calibrated in solution using the equipartition theorem (15), giving a typical spring constant of ~ 50 pN/nm. The pulling speed was set for all of the experiments at 400 nm/s. The force extension curves were fitted using the worm-like chain model of polymer elasticity (16). IGOR Pro software from WaveMetrics (Lake Oswego, OR) was used for data acquisition and analysis.

RESULTS AND DISCUSSION

Fig. 2*B* shows a characteristic force extension curve corresponding to the unfolding of $(I27)_4$ wt-EYFP $(I27)_4$. In this trace, we observe eight unfolding events at ~ 200 pN with contour length increments of $\Delta L_c \sim 28.5$ nm, corresponding to the full extension of the engineered I27 handles (13). Therefore, the unfolding peaks occurring prior to the extension of the handles must correspond to the unfolding and extension of the EYFP molecule. For example, Fig. 2*B* shows an EYFP unfolding peak

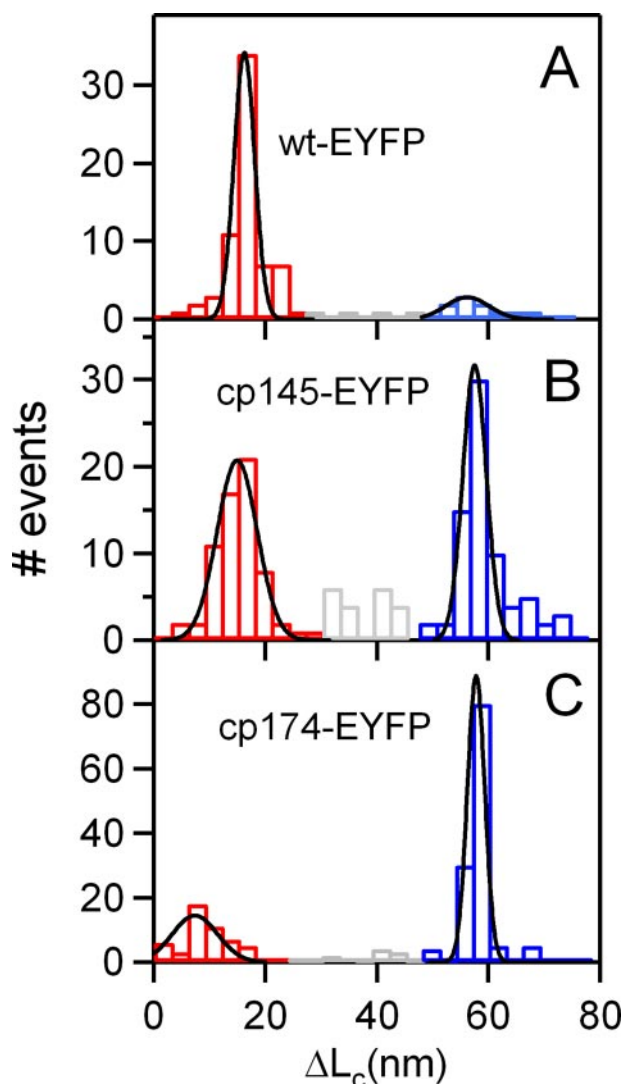


FIGURE 3. Histograms of the contour length increments observed in EYFP by taking the resting length of the protein as the starting point of unfolding. *A*, wt-EYFP shows peaks at 16 ± 3 nm (red) and at 54 ± 4 nm (blue) with $n = 80$. *B*, cp145-EYFP shows peaks at 57 ± 3 nm (blue) and 13 ± 4 nm (red) with $n = 160$. *C*, cp174-EYFP with peaks at 56 ± 2 nm (blue) and 7 ± 4 nm (red) with $n = 190$.

of 60 pN measured 79 nm before the first I27 module unfolds (Fig. 2*B*, contour length measured by fits of the worm-like chain; red lines). The contour length per amino acid was measured to be 0.4 nm (17, 18). Therefore, the complete unfolding of an EYFP protein would lead to an extension of 238×0.4 nm/amino acid ~ 95 nm. Consequently, if we take the resting length of the protein as the starting point of unfolding, the EYFP unfolding peak observed in Fig. 2*B* would be located at 16 nm from the resting length (95–79 nm).

Fig. 2, *C* and *D*, shows similar experiments using the circular permuted construct (I27)₅cp145-EYFP(I27)₄ and Fig. 2, *E* and *F*, using the circular permuted construct (I27)₅cp174-EYFP(I27)₄. Fig. 3*A* shows a histogram ($n = 80$) of all of the contour length increments measured from wt-EYFP molecule using these techniques. The figure shows a main unfolding peak at 16 ± 3 nm ($n = 67$) with a mean unfolding force of 69 ± 23 pN (Fig. 4*A*). In addition, a rare peak was observed at 54 ± 4 nm ($n = 10$) with a mean unfolding force of 122 ± 23 pN, suggest-

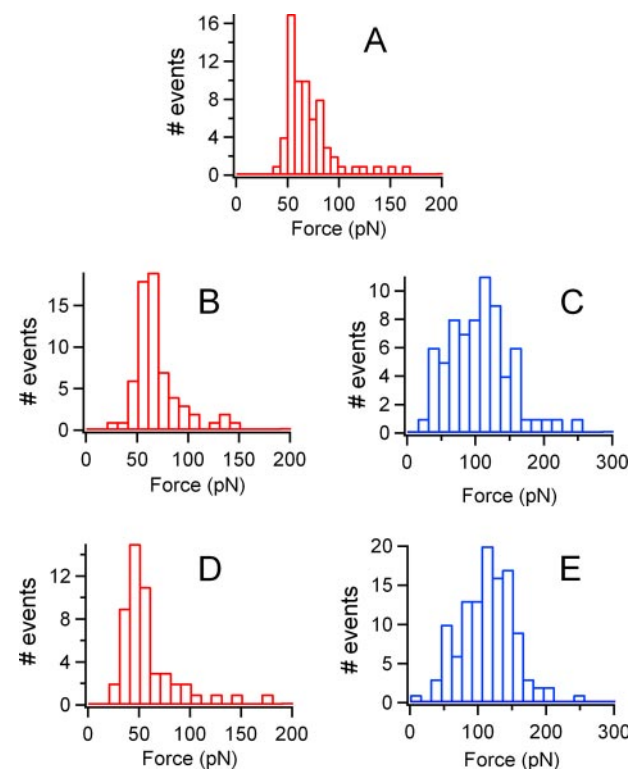


FIGURE 4. Distribution of unfolding forces. *A*, wt-EYFP with a mean force of 69 ± 23 pN. *B*, cp145-EYFP with a mean unfolding force of 68 ± 23 pN corresponding to the unfolding peak at 13 nm (see "Results and Discussion"). *C*, cp145-EYFP with a mean unfolding force of 103 ± 44 pN corresponding to the unfolding peak at 57 nm. *D*, cp174-EYFP with a mean unfolding force of 57 ± 28 pN corresponding to the peak at 7 nm. *E*, cp174-EYFP with a mean unfolding force of 112 ± 39 pN corresponding to the peak at 56 nm.

ing the presence of at least two distinct and well marked unfolding pathways. Fig. 3, *B* and *C*, shows histograms of the position of the unfolding peaks measured from cp145-EYFP (3*B*) and cp174-EYFP (3*C*). The full contour lengths of the circular permuted proteins are calculated to be 2.4 nm larger than that for wt-EYFP due to the six extra linker residues (see "Experimental Procedures"). Similar to the results obtained from the wt-EYFP, the cp145-EYFP shows two distinct unfolding pathways (Fig. 3*B*). In $\sim 40\%$ of the total number of events shown in Fig. 3*B* ($n = 160$), the unfolding peaks are found at an extension of 13 ± 4 nm with a mean unfolding force of 68 ± 23 pN (Fig. 4*B*). In 45% of the events, the unfolding peaks are found at an extension of 57 ± 3 nm and at a mean unfolding force of 103 ± 44 pN (Fig. 4*C*). The majority of the events occur individually (Fig. 2, *C* and *D*), and only in $\sim 3\%$ of the cases, both peaks are observed in the same recording (not shown). Fig. 3*C* shows a histogram of the position of the unfolding peaks obtained from cp174-EYFP ($n = 190$). In $\sim 20\%$ of the cases, we observed two consecutive unfolding peaks in the same trace (Fig. 2*F*). The first was located at 7 ± 4 nm and at mean unfolding force of 57 ± 28 pN (Fig. 4*D*), and the second was located at 56 ± 2 nm with an unfolding force of 112 ± 39 pN (Fig. 4*E*). In $\sim 78\%$ of the total number of recordings, we only observed the unfolding peak located at 56 ± 2 nm. Interestingly, the peak at 7 nm has never been observed alone in this protein.

Our results show that circular permutations of the EYFP protein retain similar unfolding peaks but alter the balance

between these pathways. The work of Dietz and Rief (8) identifies an unfolding peak in wt-GFP that is similar to the one that we observed near the resting length of the molecule (Fig. 3A). In addition, in EYFP, we then observed a second peak corresponding to an intermediate located halfway through the molecule, similar to that reported by Hara and colleagues (9, 10), although at a lower force than reported in their work.

Experimental and computational studies have shown that shearing two neighboring β -strands requires a much higher force than simply unzipping them (19–23). A close examination of the topology of EYFP (Fig. 1A) showed only two parallel neighboring β -strands, $\beta 1$ and $\beta 6$, where a shear force was required to separate them (Fig. 1B). All of the other β -strands were antiparallel and should have separated by simple unzipping. If we assume that the bonds holding together the $\beta 1$ - and $\beta 6$ -strands represent a mechanical barrier, their rupture would release at least 105 residues of the sequence in wt-EYFP and 111 residues in the circular permutant proteins. The release of these residues would result in contour length increments of the unfolding protein of ~ 53 nm (wt) and ~ 55 nm (circular permutants), in close agreement with our results. Thus, our results predict that the main mechanical barrier to unfolding the EYFP circular permutants is located in the $\beta 1$ - and $\beta 6$ -strands of the EYFP structure. This hypothesis can be verified by using proline mutations, as demonstrated previously in the identification of the mechanical transition state in the I27 module of human cardiac titin. In their study, Li *et al.* (24) show that single proline mutations inserted in the A' or G β -strands readily reduce the force required to unfold the I27 protein (24). These observations pinpoint the mechanical transition state within the I27 structure to the A' or G β -strands, which rupture in shear mode under a mechanical force.

Similarly, we have engineered a mutant form of the circular permutant cp174-EYFP replacing a glutamate by a proline in the $\beta 1$ -strand (E89P) to test the presence of a mechanical barrier between the $\beta 1$ - and $\beta 6$ -strands (Fig. 1, A and B, green star). Insertion of a proline in this site eliminates a backbone H-bond in an attempt to disrupt the mechanical transition state of EYFP. The glutamate residue in position 89 was a good candidate for this mutation, because its side chain points outwards of the β -can structure, reducing its impact in the fold of the protein. Indeed, the E89P mutation retains the same fluorescence emission (data not shown), which indicates that the protein folds into a functional structure (25). The cp174-EYFP was chosen because, due to the position of the termini, the unfolding pathway always requires the rupture by shear force of the $\beta 1$ - and $\beta 6$ -strands. Thus, the effect of the mutation would be more clearly detectable than in the other constructs.

Fig. 5 shows the experimental results obtained from the mutant E89Pcp174-EYFP protein. Similar to the cp174-EYFP, we find an unfolding peak close to the termini located at 6 ± 4 nm (Fig. 5B; $n = 46$) with a mean unfolding force of 62 ± 29 pN (not shown). However, in the majority of the traces, this unfolding peak is now observed without the presence of the intermediate at 56 nm (Fig. 5A). Thus, the probability of observing the unfolding intermediate at 56 nm was drastically reduced by the mutation (Fig. 5B, blue bars). Furthermore, when the unfolding peak at 56 nm was observed, its mean force was only 69 ± 42

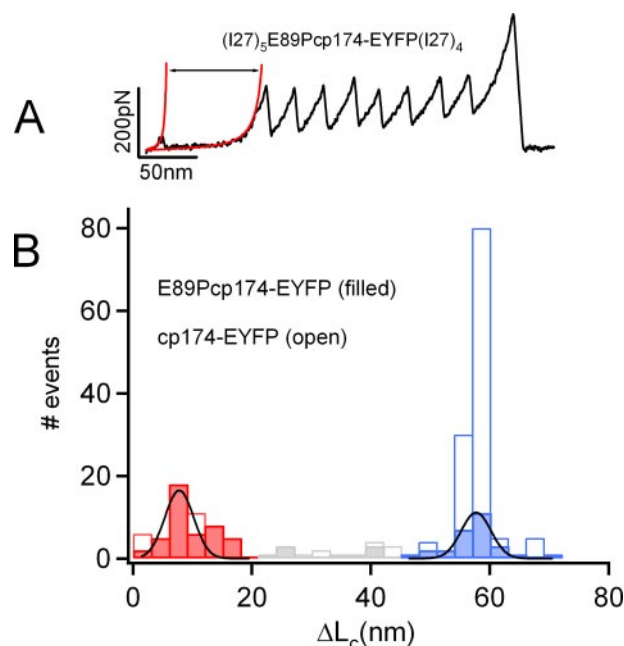


FIGURE 5. A, force extension trace for (I27)₅ E89Pcp174-EYFP(I27)₄ showing one unfolding peak at 91 ± 4 nm prior to the I27 peaks. B, comparative contour length histograms of the mutant form of cp174-EYFP, E89P (filled bars), and the non-mutated form (open bars extracted from Fig. 3) calculated by taking the resting length of the protein as the starting point of unfolding. The histogram of the E89Pcp174 form shows two peaks, one at 56 ± 4 nm (blue) and the other 6 ± 4 nm (red) with $n = 82$.

pN, which is significantly lower than that for the non-mutant form (112 pN; see above).

Our results show that the mutant E89Pcp174-EYFP protein retains unchanged both its fluorescence and also its most proximal unfolding peak (at 6 nm). These are indications that the mutation is not globally disruptive of the structure and that it acts locally. At the same time, the E89P severely reduces the mechanical strength and frequency but not the location of the most prominent unfolding peak in EYFP (located at 56 nm). These observations support our hypothesis that the principal mechanical barrier to unfolding the cp174-EYFP protein results from the mechanical interactions between the $\beta 1$ - and $\beta 6$ -strands rupturing in shear mode. Thus, it is interesting to consider the role played by the separation of the $\beta 1$ - and $\beta 6$ -strands in the wild type and the permutated forms of EYFP.

In the case of wt-EYFP, the intermediate at 56 nm, while present, was rarely observed. The main unfolding peak in the wild type form was found near the termini and close to the resting length, as noted by Dietz and Rief (8). A possible interpretation of these observations is that the preferential unfolding pathway of the wt-EYFP involves the peeling of the $\beta 1$ -strand in the first unfolding peak, thus avoiding ever reaching the antiparallel shear conformation of the $\beta 1$ - and $\beta 6$ -strands. In a small number of cases, unfolding may start by peeling $\beta 1$, allowing the protein to reach the antiparallel shear conformation of the $\beta 1$ - and $\beta 6$ -strands and showing the intermediate at the 54-nm extension. In the case of the cp145-EYFP protein, two distinct unfolding pathways are observed, the first one showing an unfolding peak at 13 nm and a second one at 57 nm. This first peak may result from peeling away strand $\beta 6$, thus preventing the formation of the intermediate at 57 nm (Fig. 1A).

Mechanical Unfolding Pathways of EYFP

The second peak (intermediate) may proceed first through β 7-strand, reaching then the shear rupture mode of the β 1- and β 6-strands. The unfolding of cp145 mainly occurs following either one or the other pathway, and only in \sim 3% of the unfolding events they occur simultaneously. The presence of a few events (12%) observed at extensions ranging between 30 and 45 nm could be attributed to other pathways revealing a higher degree of complexity in the energy landscape of this protein. In contrast to the two previous cases, the cp174-EYFP variant always shows the intermediate corresponding to the shear separation of the β 1- and β 6-strands reached at an extension of 56 nm. This is consistent with the fact that the cp174-EYFP always begins to extend far from the β 1- or β 6-strands (Fig. 1A).

Our experimental results suggest that applying force to EYFP through different positions within the protein by circular permutation results in a mechanical resistance marked by two main unfolding peaks. The weakest (between 57 and 69 pN) is always present near the termini, and it is likely because of the mechanical resistance of the local structure. A much stronger (between 103 and up to 122 pN) and better defined unfolding peak (intermediate) is apparent halfway through the protein, and it is well described by the shear rupture of β 1- and β 6-strands. This mechanical barrier has been confirmed by a proline mutation. Furthermore, our results show that the probability of attaining these unfolding transition states is greatly affected by the location of where the force is applied. Our work shows that the mechanical unfolding pathway of an EYFP protein can be deciphered by means of circular permutations and single molecule force spectroscopy.

Acknowledgment—We thank Dr. L. Dougan for critical reading of the manuscript.

REFERENCES

1. Chalfie, M., Tu, Y., Euskirchen, G., Ward, W. W., and Prasher, D. C. (1994) *Science* **263**, 802–805
2. Tsien, R. Y. (1998) *Annu. Rev. Biochem.* **67**, 509–544
3. Ormo, M., Cubitt, A. B., Kallio, K., Gross, L. A., Tsien, R. Y., and Remington, S. J. (1996) *Science* **273**, 1392–1395
4. Yang, F., Moss, L. G., and Phillips, G. N., Jr. (1996) *Nat. Biotechnol.* **14**, 1246–1251
5. Heim, R., Prasher, D. C., and Tsien, R. Y. (1994) *Proc. Natl. Acad. Sci. U. S. A.* **91**, 12501–12504
6. Baird, G. S., Zacharias, D. A., and Tsien, R. Y. (1999) *Proc. Natl. Acad. Sci. U. S. A.* **96**, 11241–11246
7. Topell, S., Hennecke, J., and Glockshuber, R. (1999) *FEBS Lett.* **457**, 283–289
8. Dietz, H., and Rief, M. (2004) *Proc. Natl. Acad. Sci. U. S. A.* **101**, 16192–16197
9. Wang, T., Nakajima, K., Kogure, T., Yokokawa, S., Miyawaki, A., and Hara, M. (2004) *Jpn. J. Appl. Phys.* **43**, 5520–5523
10. Wang, T., Nakajima, K., Miyawaki, A., and Hara, M. (2005) *Ultramicroscopy* **105**, 90–95
11. Wang, T., Sakai, Y., Nakajima, K., Miyawaki, A., Ito, K., and Hara, M. (2005) *Colloids Surf. B* **40**, 183–187
12. Wachter, R. M., Elsliger, M. A., Kallio, K., Hanson, G. T., and Remington, S. J. (1998) *Structure* **6**, 1267–1277
13. Carrion-Vazquez, M., Oberhauser, A. F., Fowler, S. B., Marszalek, P. E., Broedel, S. E., Clarke, J., and Fernandez, J. M. (1999) *Proc. Natl. Acad. Sci. U. S. A.* **96**, 3694–3699
14. Oberhauser, A. F., Marszalek, P. E., Erickson, H. P., and Fernandez, J. M. (1998) *Nature* **393**, 181–185
15. Florin, E. L., Rief, M., Lehmann, H., Ludwig, M., Dornmair, C., Moy, V. T., and Gaub, H. E. (1995) *Biosens. Bioelectr.* **10**, 895–901
16. Marko, J. F., and Siggia, E. D. (1995) *Macromolecules* **28**, 8759–8770
17. Ainarapu, S. R., Brujic, J., Huang, H. H., Wiita, A. P., Lu, H., Li, L., Walther, K. A., Carrion-Vazquez, M., Li, H., and Fernandez, J. M. (2007) *Biophys. J.* **92**, 1–9
18. Carrion-Vazquez, M., Marszalek, P. E., Oberhauser, A. F., and Fernandez, J. M. (1999) *Proc. Natl. Acad. Sci. U. S. A.* **96**, 11288–11292
19. Marszalek, P. E., Lu, H., Li, H., Carrion-Vazquez, M., Oberhauser, A. F., Schulten, K., and Fernandez, J. M. (1999) *Nature* **402**, 100–103
20. West, D. K., Brockwell, D. J., Olmsted, P. D., Radford, S. E., and Paci, E. (2006) *Biophys. J.* **90**, 287–297
21. Cao, Y., Lam, C., Wang, M., and Li, H. (2006) *Angew. Chem. Int. Ed. Engl.* **45**, 642–645
22. Lu, H., Isralevitz, B., Krammer, A., Vogel, V., and Schulten, K. (1998) *Biophys. J.* **75**, 662–671
23. Gao, M., Craig, D., Vogel, V., and Schulten, K. (2002) *J. Mol. Biol.* **323**, 939–950
24. Li, H., Carrion-Vazquez, M., Oberhauser, A. F., Marszalek, P. E., and Fernandez, J. M. (2000) *Nat. Struct. Biol.* **7**, 1117–1120
25. Fukuda, H., Arai, M., and Kuwajima, K. (2000) *Biochemistry* **39**, 12025–12032